Inorganic Chemistry

Article

pubs.acs.org/IC

Solution-Based Synthesis of GeTe Octahedra at Low Temperature

Stephan Schulz,*[,†] Stefan Heimann,[†] Kevin Kaiser,[†] Oleg Prymak,[†] Wilfried Assenmacher,[‡] Jörg Thomas Brüggemann,[§] Bert Mallick,[§] and Anja-Verena Mudring[§,⊥]

[†]Institute of Inorganic Chemistry and Center for Nanointegration Duisburg-Essen (CENIDE), University of Duisburg-Essen, Universitätsstraße 5-7, D-45117 Essen, Germany

[‡]Institute of Inorganic Chemistry, University of Bonn, Römerstraße 164, D-53117 Bonn, Germany

[§]Inorganic Chemistry III—Materials Engineering and Characterization, Ruhr-University Bochum, 44780 Bochum, Germany

[⊥]Materials Science and Engineering, Iowa State University, Ames, Iowa 50010, United States

Supporting Information

ABSTRACT: GeTe octahedra were prepared by reaction of equimolar amounts of $GeCl_2$·dioxane and $Te(SiEt_3)_2$ in oleylamine, whereas a slight excess of the Te precursor yielded GeTe octahedra decorated with elemental Te nanowires, which can be removed by washing with TOP. The mechanism of the GeTe formation is strongly influenced by the solvent. The expected elimination of Et_3SiCl (dehalosilylation) only occurred in aprotic solvents, whereas $Te(SiEt_3)_2$ was found to react with primary and secondary amines with formation of silylamines. Temperature-dependent studies on the reaction in oleylamine showed that crystalline GeTe particles are formed at temperatures higher than 140 °C. XRD, SAED, and HRTEM studies proved the formation of rhombohedral GeTe nanoparticles. These findings were confirmed by a single-crystal and powder X-ray analysis. The rhombohedral structure modification was found, and the structure was solved in the acentric space group *R*3*m*.

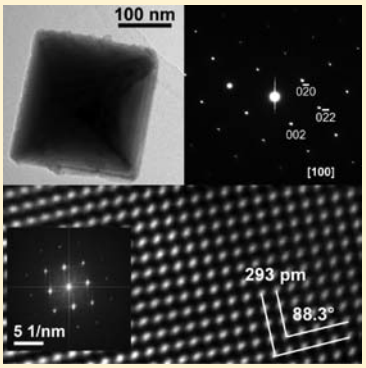

INTRODUCTION

Nanostructured metal chalcogenides have received increasing interest over the past decade due to their possible technical applications in energy devices such as fuel and solar cells, light-emitting diodes, Li-ion batteries, and thermoelectric devices.[1] Germanium telluride, GeTe, and the related GST compounds ($Ge_2Sb_2Te_5$) are interesting phase change materials (PCM).[2−6] GST compounds typically crystallize either in a metastable face centered cubic (*C*) phase or in the stable rhombohedral (*R*) or hexagonal (*H*) phase. For materials belonging to these classes reversible amorphous-to-crystalline phase transitions are frequently observed,[7−12] which can be triggered thermally or electrically. Upon crystallization, the conductivity and reflectivity of GeTe significantly change, hence rendering this material a very promising candidate in nonvolatile phase change random access memory (PCRAM) such as CDs or DVDs.[13,14] The ferroelectric phase change of GeTe results from a distinctive structural change between the nonpolar rock salt structure to the polar rhombohedral phase. This symmetry-breaking structural distortion occurs below 350 °C.[15] Furthermore, GeTe is well known to exhibit thermoelectric properties.[16]

Nanosized PCM materials such as GeTe nanoparticles are very interesting because of the well-known influence of the reduced dimensionality of a given material on its physical properties such as melting points or crystallization properties.[17−22] Since GeTe nanoparticles are expected to improve device performances,[23] the interest in suitable precursors for the size- and shape-selective synthesis of GeTe nanocrystals has remarkably increased in recent years, and several general reaction pathways have been established.[24] GeTe nanowires containing a large excess of elemental tellurium were formed in high-boiling organic solvents via seed-mediated growth using Bi nanoparticles,[25] whereas GeTe nanowires with uniform diameter distributions were grown on the basis of the VLS mechanism.[26] Wet chemical (colloidal) routes also gave access to amorphous and crystalline GeTe nanoparticles with distinctive shape and size. Reactions of GeI_2 with TOPTe in the presence of tri-*n*-octylphosphine (TOP), tri-*n*-octylphosphine oxid (TOPO), and dodecanethiol at 250 °C yielded amorphous GeTe nanoparticles, whose sizes ranged from 1.7 to 5 nm.[23] A strong correlation between the crystal size and the crystallization temperature was observed, with a decreasing particle size leading to an increase in crystallization temperature. While for bulk GeTe an amorphous-to-crystalline phase transition was observed at about 170 °C,[27] 1.8 nm sized GeTe nanoparticles started to crystallize not before 240 °C.[23] Crystalline GeTe nanoparticles were also obtained from the reaction of $Ge[N(SiMe_3)_2]_2$ and TOPTe in 1-octadecene at 200 °C in the presence of oleylamine and dodecanethiol, whereas amorphous GeTe particles were formed in the absence of dodecanethiol at reaction temperatures below 170 °C.[27] Increasing reaction times produced larger, polydisperse nanoparticles (9.0−27.8 nm). Alivisatos et al. recently reported on

Received: September 13, 2013
Published: November 22, 2013

   dx.doi.org/10.1021/ic402266j | *Inorg. Chem.* 2013, 52, 14326−14333

the synthesis of GeTe nanocrystals with variable sizes using germanium precursors of different reactivity.[28] The reaction of $Ge[N(SiMe_3)_2]_2$ with TOPTe in 1-dodecanethiol and an excess of TOP at 250 °C yielded crystalline GeTe nanoparticles with an average size of almost 9 nm, whereas nanoparticles with an average diameter of roughly 17 nm were obtained at 250 °C in the presence of oleylamine.[29] In contrast, the reaction of the less reactive $GeCl_2$·dioxane with TOPTe and 1-dodecanethiol at 180 °C produced significantly larger GeTe nanocrystals (~100 nm). Micron-sized crystalline GeTe nanoparticles of octahedral shape with terminal {111} facets decorated with vertically aligned arrays of Te nanowires were synthesized by reaction of Ph_2Ge and TOPTe under supercritical conditions in hexane (460 °C, 13.6 MPa).[30] In contrast, GeTe cubes with an average edge length of 1.0 μm were obtained from reactions of GeI_2 with *tert*-butylamine-borane (TBAB) in the presence of TOPTe at 180 °C.[31] In this reaction, GeI_2 is first reduced to elemental Ge^0, which is then consequently oxidized by TOPTe to give GeTe and TOP.

While these synthetic procedures used TOPTe without exception as Te precursor, we became interested in alternate Te precursors for the low-temperature synthesis of Te-based materials. Bis(trialkylsilyl)telluranes $Ti(SiR_3)_2$ (R = Me, Et, ...) have been identified as powerful Te transfer reagents in metal organic chemistry for the synthesis of Te-containing main group and transition metal complexes.[32−37] Moreover, they have recently been used in atomic layer deposition (ALD) deposition of Te-based materials films such as Sb_2Te_3.[38−40] While this work was in progress, Kim et al. reported on the time-dependent reaction of $GeCl_2$·dioxane with $Te(SiEt_3)_2$ in TOP/TOPO at 250 °C, yielding GeTe nanoparticles of different sizes by a ligand exchange reaction.[41] While short reaction times (<10 min) yielded amorphous powders, elongated reaction times (30, 60 min) gave faceted, almost monodisperse GeTe cubes (350 nm size). In addition, Buck et al. reported very recently on the polymer-assisted synthesis of GeTe nanoparticles of octahedral faceted shape.[42]

We now report herein our detailed studies on the reaction of $GeCl_2$·dioxane with $Te(SiEt_3)_2$ in the absence of any reducing agent. The role of the solvent and the influence of reaction time and temperature were studied in detail. In addition, the single-crystal X-ray analysis of α-GeTe is reported.

EXPERIMENTAL SECTION

Materials. $GeCl_2$·dioxane (ABCR) was used as received, 1,3-diisopropylbenzene (DIPB, Sigma-Aldrich) was carefully dried over Na/K alloy and oleylamine (Acros), hexadecylamine (Acros), 1-hexadecanethiol (Sigma-Aldrich), tri-*n*-octylphosphine (Sigma-Aldrich), di-*n*-octylamine (Acros), and tri-*n*-octylamine (Acros) were degassed prior to use. $Te(SiEt_3)_2$ was synthesized according to a literature method.[43] All syntheses were performed under an argon atmosphere using standard Schlenk techniques.

Synthesis of GeTe Particles. $GeCl_2$·dioxane (150 mg, 0.65 mmol) was suspended in 20 mL of the solvent (oleylamine, hexadecylamine, 1-hexadecanethiol, DIPB, tri-*n*-octylamine) and heated to 150 °C. $Te(SiEt_3)_2$ (200 mg, 0.56 mmol) was injected into the yellow suspension, immediately giving a black suspension, which was stirred for an additional 4 h. The reaction mixture was allowed to cool to ambient temperature, and the GeTe particles were isolated by centrifugation, repeatedly washed (three times) with $CHCl_3$, and dried under vacuum.

Thermal Analysis. Thermogravimetric analysis (TGA)/differential thermal analysis (DTA) was performed on a Mettler Toledo Star 1 machine under Ar flow (heating rate 2 °C min^{-1}).

Single-Crystal X-ray Diffraction. Single-crystal X-ray analysis was performed on a Stoe IPDS I diffractometer (Mo Kα radiation, λ = 0.71073 Å). Crystallographic data were collected at 80(2) and 298(2) K. The structure was solved by direct methods (SIR-92) and refined anisotropically by full-matrix least-squares on F^2 (SHELXL-97).[44,45] Absorption corrections were performed semiempirically by approximating the true crystal size and shape from equivalent reflections (Stoe X-Shape).

X-ray Powder Diffraction (XRD). XRD patterns were obtained at ambient temperature, i.e., at 25 ± 2 °C, using a Bruker D8 Advance powder diffractometer in Bragg−Brentano mode with Cu Kα radiation (λ = 1.5418 Å, 40 kV, and 40 mA). The powder samples were investigated in the range of 5 to 90° 2θ with a step size of 0.01° 2θ and a counting time of 0.3 s. For each Rietveld refinement, performed with the program package TOPAS 4.2 from Bruker, the instrumental correction as determined with a standard powder sample LaB_6 from NIST (National Institute of Standards and Technology) as standard reference material (SRM 660b) was taken into account.

SEM Analysis. Scanning electron microscopy (SEM) studies were carried out on a Jeol JSM 6510 equipped with an energy-dispersive X-ray spectroscopy (EDX) device (Bruker Quantax 400).

TEM Analysis. Transmission electron microscopy (TEM) studies were performed on a Philips CM300UT-FEG operated at 300 keV and equipped with a germanium EDS detector (ThermoScientific NSS6) for energy-dispersive X-ray spectroscopy (EDS) analysis. The samples were prepared on perforated carbon foils without further grinding.

RESULTS AND DISCUSSION

The reaction of $GeCl_2$·dioxane with $Te(SiEt_3)_2$ was monitored by ^1H and ^{13}C NMR spectroscopy (Figure 1, Supporting Information). Temperature-dependent spectra, which were recorded in C_6D_6 and in THF-d_8 solutions, clearly showed the formation of Et_3SiCl starting at 25 °C. Comparable findings were reported by Leskelä et al. for the ALD deposition of metal chalcogenide thin films by reaction of $Te(SiEt_3)_2$ and metal halides such as $SbCl_3$ and $GeCl_2$·dioxane, respectively.[38,39,46]

Scheme 1. Reaction of $GeCl_2$·dioxane and $Te(SiEt_3)_2$ in C_6D_6 and THF-d_8

$$GeCl_2\cdot\text{dioxane} + Te(SiEt_3)_2 \longrightarrow GeTe + 2Et_3SiCl$$

In contrast, the reaction of $GeCl_2$·dioxane and $Te(SiEt_3)_2$ in oleylamine did not proceed with elimination of Et_3SiCl (Figure 2, Supporting Information). Oleylamine is known to serve as capping and reducing agent,[47] and Alivisatos et al. reported on reactions of $GeCl_2$·dioxane and $Ge[N(SiMe_3)_2]_2$ with primary amines (oleylamine) and alkanethiols (1-dodecanethiol), which proceeded at elevated temperatures with subsequent formation of Ge(0) nanoparticles.[29] The lower reduction rate of $GeCl_2$·dioxane compared to $Ge[N(SiMe_3)_2]_2$ resulted in lower Ge(0) particle nucleation rates and increasing nanoparticle sizes. However, we proved by ^1H NMR spectroscopy (Figure 2, Supporting Information) that oleylamine reacts immediately with $Te(SiEt_3)_2$ at ambient temperature with formation of silylamine (oleylN(H)$SiEt_3$) and subsequent formation of a deep red solution, which is characteristic for the formation of tellurium polyanions such as the $[Te_4]^{2-}$ dianion.[48] According to these findings, we assume that *in situ* formed Te−H species, which are strong acids, are deprotonated by the excess amine base. Tellurium polyanions then react with $GeCl_2$·dioxane with formation of GeTe. According to these studies, oleylamine has to be considered rather as a reagent that has a strong influence on the whole reaction mechanism than as a simple capping agent.

dx.doi.org/10.1021/ic402266j | Inorg. Chem. 2013, 52, 14326−14333

Reactions of $Te(SiEt_3)_2$ and $GeCl_2$·dioxane were investigated in noncoordinating, aprotic (DIPB) and in coordinating, protic solvents (oleylamine) at 160 °C in order to further investigate the role of the solvent on the particle composition and morphology.

Scanning electron microscopy (SEM) images of the resulting materials showed the formation of largely agglomerated, noncrystalline particles in DIPB, whereas GeTe particles of octahedral shape were obtained in oleylamine (Figure 1). The

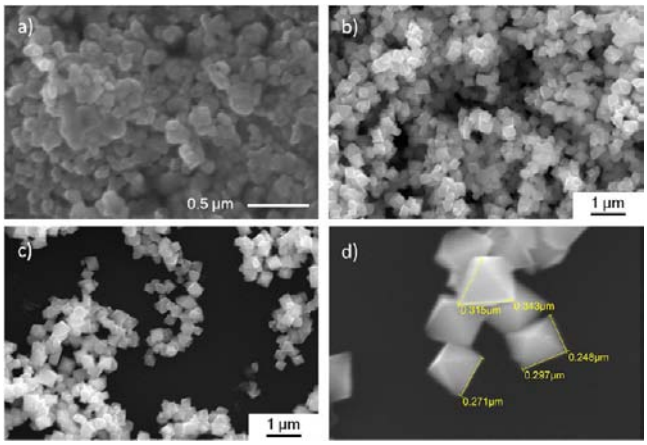

Figure 1. SEM micrographs of GeTe particles as obtained in (a) DIPB and in (b–d) oleylamine at 160 °C.

elemental compositions (Ge, Te) in both materials are in accordance with the formation of pure GeTe. The edge lengths of the GeTe octahedra ranged from 250 to 350 nm. This is significantly smaller compared to the octahedral GeTe crystallites synthesized in supercritical hexane at significantly higher reaction temperatures (460 °C), which showed edge lengths of about 1 μm.[30] Moreover, these octahedra were largely decorated with elemental tellurium nanowires. Even larger GeTe octahedra of several micrometers were obtained from a vapor transport process.[49]

Transmission electron microscopy (TEM) investigations (Figure 2) of the octahedral-shaped GeTe particles confirmed the unimodal size distribution and edge length of 300 nm as found by SEM and revealed all particles to be crystalline.

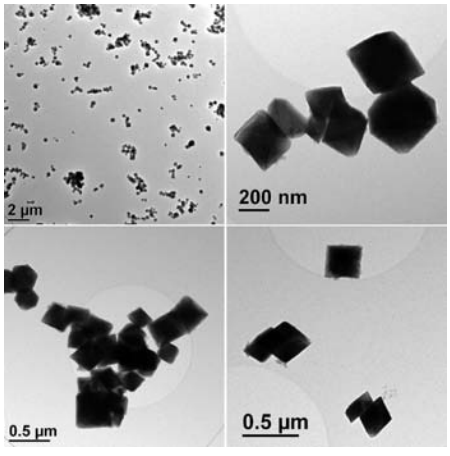

Figure 2. TEM images of GeTe octahedra as obtained at 160 °C in oleylamine.

The composition of the GeTe octahedra from EDS nanobeam analysis of 20 different crystals was determined with a Ge:Te ratio of 48:52 on average with a standard deviation of 2 for both elements. This agrees, within experimental error, with the expected composition of GeTe. Electron diffraction (ED) patterns from different zone axis orientations (given in the Supporting Information) can be indexed consistently with a rhombohedral cell, yielding lattice parameters a = 5.98 Å and α = 88.3°, which are in good agreement with α-GeTe and with the results from powder X-ray diffraction (PXRD) of this sample as shown in Figure 5. It is

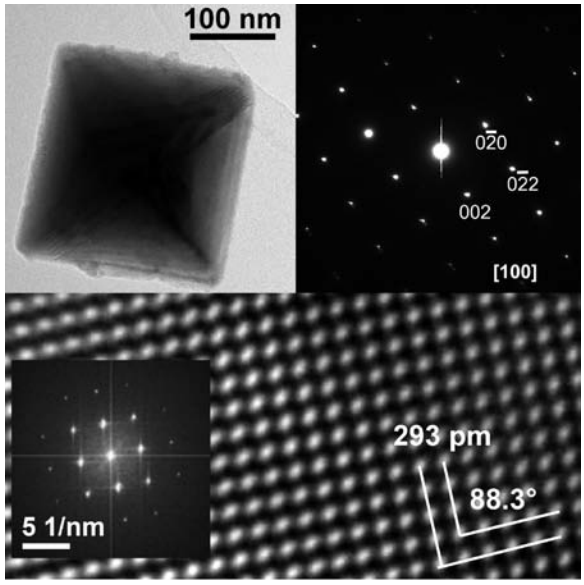

Figure 3. (Top) TEM bright-field image of a GeTe octahedron in [100] orientation and corresponding ED pattern. (Bottom) HRTEM image and corresponding FT as inset. GeTe as-obtained at 160 °C in oleylamine.

more convenient to describe α-GeTe with the rhombohedral cell in space group $R3m$ (no. 160) than with a hexagonal R cell to show the close relationship to the rock salt structure. Figure 3 shows a GeTe crystal viewed along the [100] zone axis with the corresponding pattern in the same orientation. Obviously,

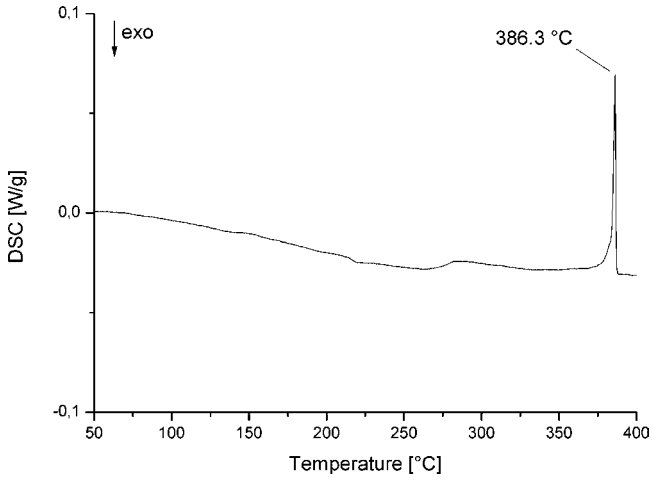

Figure 4. Differential scanning calorimetry (DSC) curve of freshly prepared GeTe octahedra.

dx.doi.org/10.1021/ic402266j | Inorg. Chem. 2013, 52, 14326–14333

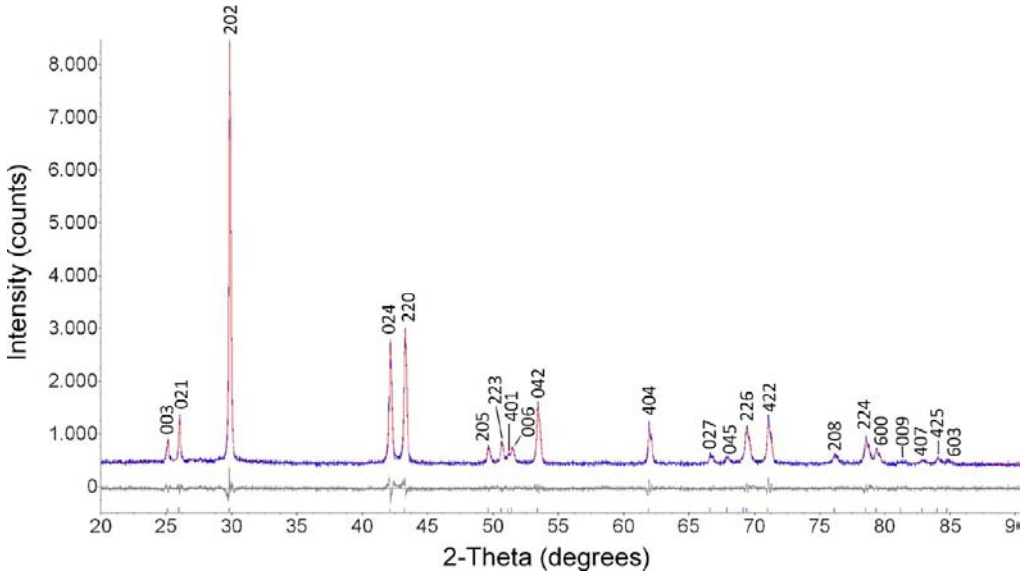

Figure 5. PXRD pattern of GeTe nanoparticles formed at 150 °C after 4 h including the results from Rietfeld refinement as difference plot (R_wp = 5.02).

the corners of the pseudo-octahedra grow in the ⟨100⟩ and the edges are in the ⟨110⟩ direction. The triangular faces are in the ⟨111⟩ direction (cf. Supporting Information). The growing directions are the same as for octahedra of fcc crystals. Parallel lines indicate the {002} lattice fringes with a *d*-value of 293 pm in the HRTEM image. The slight distortion from the cubic symmetry is reflected by the angle of 88.3° between the {002} lattice fringes.

Our TEM results are in excellent agreement with the findings of Kim et al.[41] on octahedral-shaped GeTe nanocrystals. They described their particles to have a unimodal distribution (average value 337 nm) and a composition of 47:53 and 56.6:43.4 Ge:Te ratios from two EDS measurements. HRTEM exhibits well-resolved 2D lattice fringes with plane spacings of 222 pm, which correspond to lattice planes of {024} in hexagonal *R* GeTe. These findings are within the error of ED and consistent with the *d*-value of {022} fringes in rhombohedral setting as observed in our samples. Recently, Buck et al. reported on the polymer-assisted synthesis of GeTe nanoparticles of octahedral-faceted shape.[42] The lattice parameters of the rhombohedral GeTe nanoparticles were proven by ring diffraction patterns from selected area electron diffraction (SAED) of a number of crystals. The growing direction was deduced from HRTEM to be ⟨111⟩ for the octahedral planes, and the composition as derived from EDS was found to be $Ge_{52}Te_{48}$.

The TGA/DTA analysis (Figure 3, Supporting Information) of the isolated GeTe octahedra as obtained from the reaction in oleylamine at 160 °C showed an endothermic peak at 716 °C, which is slightly lower than that reported by Kim et al. (721.8°),[41] whereas the melting point of bulk GeTe is significantly higher (725 °C).[50] A TGA experiment showed a weight loss of only 1.2% up to a temperature of 500 °C, which is a good indicator for the purity of the GeTe microcrystals. More substantial weight loss started at 600 °C due to sublimation of GeTe. A DSC study (Figure 4) showed a first-order solid−solid phase transformation at 386 °C, which is in between the temperatures previously reported (350 °C,[15] 402 °C[51]).

The PXRD diffraction pattern (Figure 5) of GeTe obtained at 160 °C in oleylamine corresponds very well to nanocrystalline *α*-GeTe in space group *R*3*m*. The calculated lattice parameters (a = 8.3642(1) Å, c = 10.6524(3) Å, V = 645.40(3) Å^3) agree very well with those obtained from the TEM studies as well as the results of the single-crystal X-ray structure analysis. The data are also in very good agreement with JCPDS No. 47-1079.[52] The calculated density of the unit cell (6.18 g/cm^3) agrees well with that of bulk *α*-GeTe (6.14 g/cm^3). The determined crystallite size (using the Scherrer equation) of 160 nm confirms the nanostructure of the produced GeTe particles and corresponds to the values of the TEM studies. In addition, microstrain (ε = 0.07%) as another influential effect on the peak broadening in the diffractogram was also detected ("Williamson−Hall plot", see Figures S4 in the Supporting Information). The calculated texture coefficients (relationship defined by Barret and Massalski)[66] for the first 11 *hkl* values did not show any sign of texture effects (see Table S1 in the Supporting Information).

Since the results of the reaction of $GeCl_2$·dioxane and $Te(SiEt_3)_2$ in oleylamine were much more promising than those in DIPB, we focused on this reaction and particularly investigated the role of reaction time, reaction temperature, and solvent in detail.

Growth Mechanism. Reactions between $GeCl_2$·dioxane and $Te(SiEt_3)_2$ at 150 °C in oleylamine were carried out to determine the starting point of crystallization and formation of octahedral GeTe. Figure 6 shows SEM images of the solid precipitate obtained after different reaction times, which show the formation of crystalline GeTe octahedra 60 min after starting the reaction, whereas shorter reaction times produced particles without defined shape, most likely much smaller particles whose shape could not be resolved precisely. These findings point to a thermodynamically driven Ostwald-ripening-type crystal growth process, in which large numbers of small GeTe crystals of heterogeneous shape over time grow to fewer larger crystals with well-defined morphology and shape in order to decrease their energy. The formation of a large number of small GeTe crystals requires a spontaneous precipitation of crystal seeds by a very fast reaction between $GeCl_2$·dioxane and

dx.doi.org/10.1021/ic402266j | *Inorg. Chem.* 2013, 52, 14326−14333

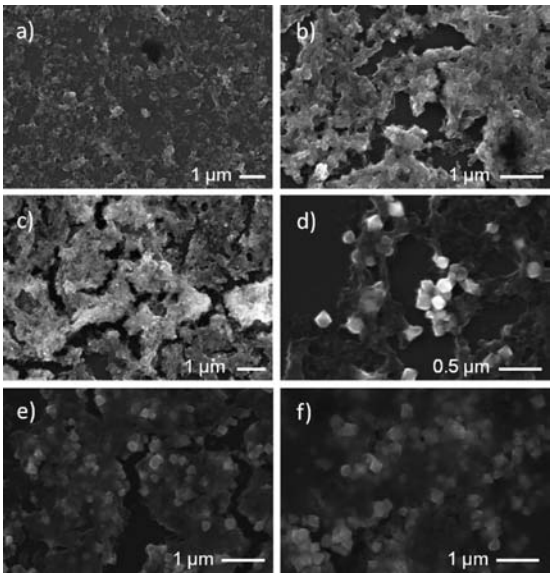

Figure 6. SEM micrographs of time-dependent formation of GeTe octahedra at 150 °C in oleylamine after (a) 5, (b) 15, (c) 30, (d) 60, (e) 120, and (f) 240 min.

$Te(SiEt_3)_2$, hence producing a large number of crystal seeds, which is very likely under these specific conditions according to our NMR studies.

Role of Reaction Temperature. The reaction temperature was lowered to 100 °C in order to verify its influence on the size, shape, and crystallinity of the GeTe particles. The formation of octahedral GeTe particles was observed starting at 140 °C (Figure 7), whereas lower reaction temperatures gave only materials with unspecific morphologies. XRD studies proved that the formation of crystalline GeTe particles started at 140 °C. The size of the crystalline GeTe particles formed at 160 °C is larger than that of the particles formed at 140 °C, as can be derived from the sharper reflexes. Reactions performed at 180 °C also gave GeTe particles, whose size and shape were comparable to those obtained at 160 °C. These findings somehow correlate with those of previous studies, in which the amorphous-to-crystalline phase transition for GeTe thin films was found to occur at 145 °C,[53,54] whereas bulk GeTe started to crystallize at roughly 180 °C.[55] However, this finding has to be considered as rather coincidentally since the solution-based growth of crystalline GeTe particles kinetically differs from the reorganization of solid GeTe from the metastable amorphous state to the crystalline state.

Role of $Te(SiEt_3)_2$ Concentration. The reaction of an excess of $Te(SiEt_3)_2$ with $GeCl_2$·dioxane at 140 °C in oleylamine proceeded with formation of α-GeTe (JCPDS Card No. 47-1079) and crystalline hexagonal Te (JCPDS Card No. 36-1452) according to powder X-ray diffraction studies (Figure 8).

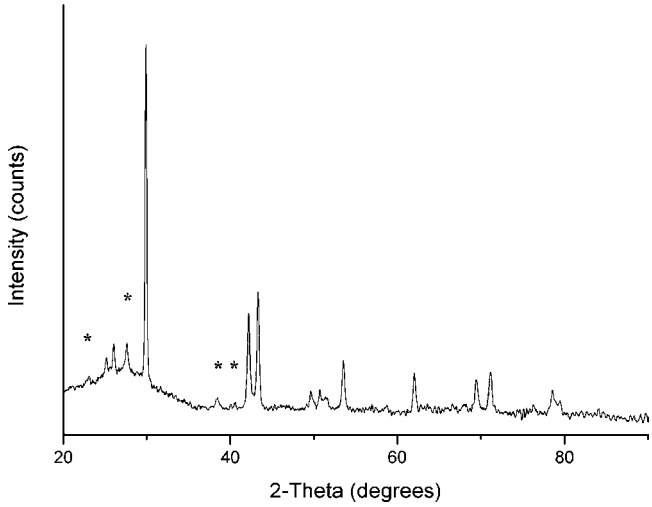

Figure 8. XRD pattern of Te-covered GeTe particles. (*)-labeled reflexes correspond to trigonal Te ($P3_121$ (No. 152), JCPDS No. 36-1452).

TEM studies revealed the formation of GeTe octahedra, whose surface is covered with Te nanowires (Figure 9a, b).

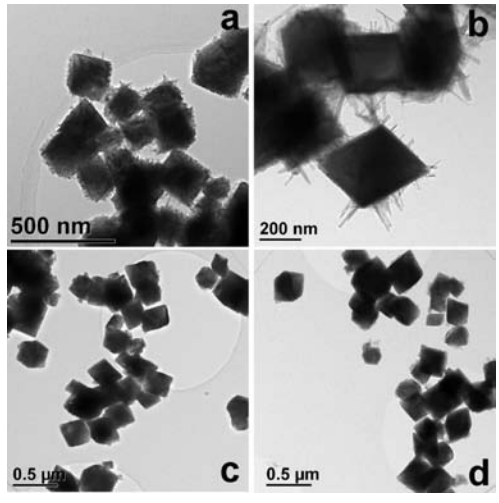

Figure 9. TEM micrographs of GeTe octahedra (a, b) decorated with elemental Te nanowires and (c, d) after washing with TOP.

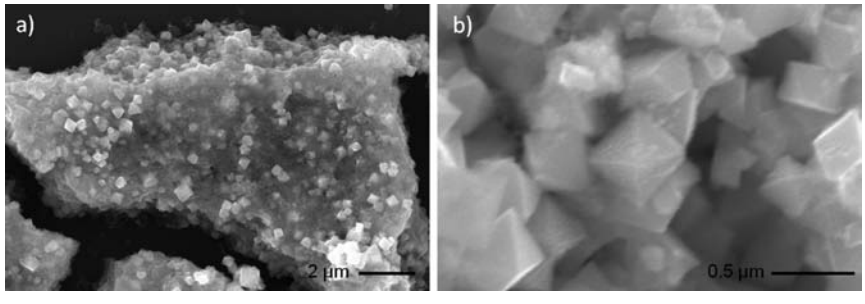

Figure 7. SEM micrographs showing the formation of GeTe octahedra at (a) 140 °C and (b) 150 °C.

dx.doi.org/10.1021/ic402266j | Inorg. Chem. 2013, 52, 14326−14333

Te-decorated GeTe particles were previously obtained by Korgel et al. in reactions of diphenyl germane ($GePh_2$) with TOPTe in supercritical hexane at 460 °C in the presence of octanol, oleic acid, or isoprene,[30] whereas hexadecanethiol completely quenched the Te nanowire formation. The formation of the Te@GeTe particles was explained by initial formation of the GeTe core, from which the Te nanowires grew off their faceted surfaces. Even though the exact mechanism of the Te nanowire formation remained unclear, the authors suggested that the additives either modify the reactant decomposition kinetics or influence the reactivity of the particle surfaces due to the binding/passivation with different capping agents. However, we observed that the Te wires can be removed by washing the Te@GeTe particles with TOP, resulting in the formation of TOPTe (Figure 9c,d).

Role of Solvent. To verify the specific role of the solvent, we further investigated the reaction of $GeCl_2$·dioxane and $Te(SiEt_3)_2$ in hexadecylamine, di-*n*-octylamine, tri-*n*-octylamine, and 1-hexadecanethiol, respectively.

Crystalline GeTe particles of octahedral shape were obtained in hexadecylamine and di-*n*-octylamine, whereas the reactions in tri-*n*-octylamine and 1-hexadecanethiol preferably occurred with formation of elemental tellurium (Figure 10). In particular

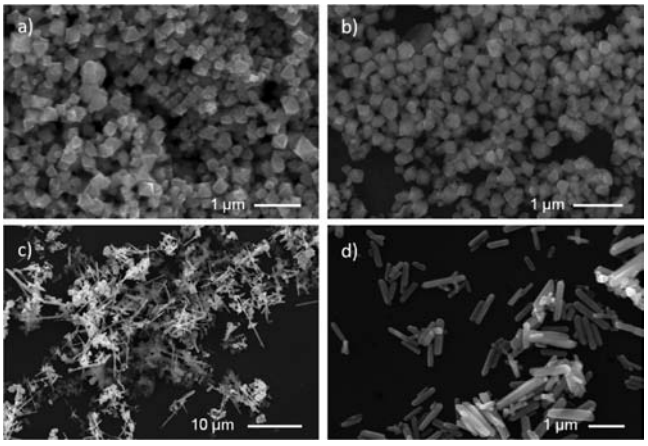

Figure 10. SEM micrographs of (a) GeTe octahedra as-formed in hexadecylamine and (b) di-*n*-octylamine; Te particles as-obtained from (c) tri-*n*-octylamine, and (d) 1-hexadecanethiol.

the formation of Te crystallites in the presence of hexadecanethiol is somewhat surprising, since Milliron et al. reported on the synthesis of GeTe nanoparticles with controlled size and morphology only in the presence of dodecanethiol,[23] while Korgel et al. reported that hexadecanethiol quenches the formation of elemental Te nanowires.[30] These findings also demonstrate that the initial formation of Te polyanions by amination of $Te(SiEt_3)_2$, which proceeds only with primary and secondary amines, seems to play a key role in the reaction mechanism of the GeTe particle formation. In summary, we believe that protic, strongly coordinating solvents are essential for the formation of GeTe nanoparticles with defined size and morphology.

Single-Crystal Analysis. Bulk GeTe has long served as a prototype for phase change materials as a result of its simple composition and structure.[53,56] Amorphous GeTe is a semiconductor with a band gap of 0.8 eV and an electrical resistivity of 10^3 Ωcm, whereas both values changes dramatically upon crystallization (0.1 eV, 10^{-4} Ωcm).[57] As a consequence, the structure of GeTe has been largely investigated in the past. Amorphous GeTe becomes crystalline at roughly 180 °C. A rhombohedral GeTe phase, α-GeTe, is formed, which further undergoes a phase transition to the more symmetric high-temperature rock-salt (NaCl-type) phase, which is stable only above 400 °C. The phase transition was found to occur at 350 °C;[53] in other reports a transition temperature of roughly 400 °C is reported.[51] However, the structure reports are contradictory. There is little doubt that the structure of α-GeTe is related to its high temperature modification β-GeTe, which crystallizes in the NaCl type of structure. Upon cooling, a distortion along the 3-fold axis occurs and the crystal system undergoes a transition from cubic to rhombohedral. For the rhombohedral modification structure solutions have been reported in the acentric space group $R3m$ with (hexagonal) lattice parameters of a = 4.2 Å and c = 10.7 Å.[58,59] However, also reports of a unit cell with a 4-times larger volume and double a-axis (a = 8.3 Å and c = 10.7 Å)[60,61] can be found, and the structure has been solved in the centric space group $R\bar{3}m$[62−65] as well as in its acentric counterpart $R3m$.[58]

Single GeTe crystals were grown from freshly prepared GeTe upon slow sublimation at 650 °C and 10^{-3} mbar. Crystals of almost perfect octahedral morphology up to 200 μm in size were obtained within 16 h (Figure 11).

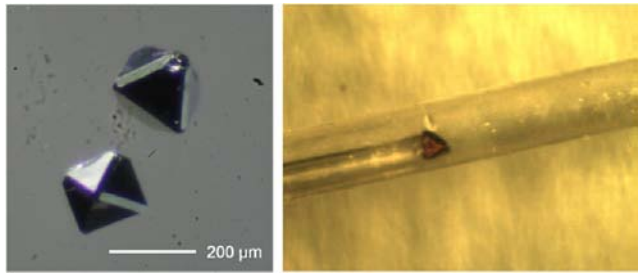

Figure 11. Picture of GeTe single crystals as obtained by slow sublimation (left) and the crystal used for X-ray analysis (right).

Single X-ray structure analysis at low and room temperature confirmed the larger cell with a = 8.471(5) Å and c = 10.392(6) Å, which yields a c/a ratio of 1.226 and a volume of V = 645.8(7) Å^3 at 80(2) K and a = 8.396(2) Å and c = 10.637(3) Å with a c/a ratio of 1.267 at 298(2) K with a volume of V = 649.43(2) Å^3 (for details on the data collection and structure solution see the Supporting Information). On the basis of the appearance of weak reflections the smaller cell with half the a-axis had to be dismissed. Also a structure solution in the smaller unit cell was unstable, and comparison of the calculated powder pattern based on this solution and the recorded powder pattern clearly rule out the smaller unit cell (Figure 5 and the Supporting Information).

Structure solution in the larger unit cell succeeded in both the acentric space group $R3m$ and the centric space group $R\bar{3}m$. The R-values as well as the goodness of fit for a structure solution as an inversion twin in the acentric space group were noticeably smaller. A clear proof why a structure report in the acentric space group should be preferred over the centric becomes clear when analyzing the anisotropic displacement parameters (Figure 12).

■ CONCLUSIONS

Nanosized GeTe octahedra were obtained from the reaction of $GeCl_2$·dioxane and $Te(SiEt_3)_2$ at temperatures as low as 160

dx.doi.org/10.1021/ic402266j | Inorg. Chem. 2013, 52, 14326−14333

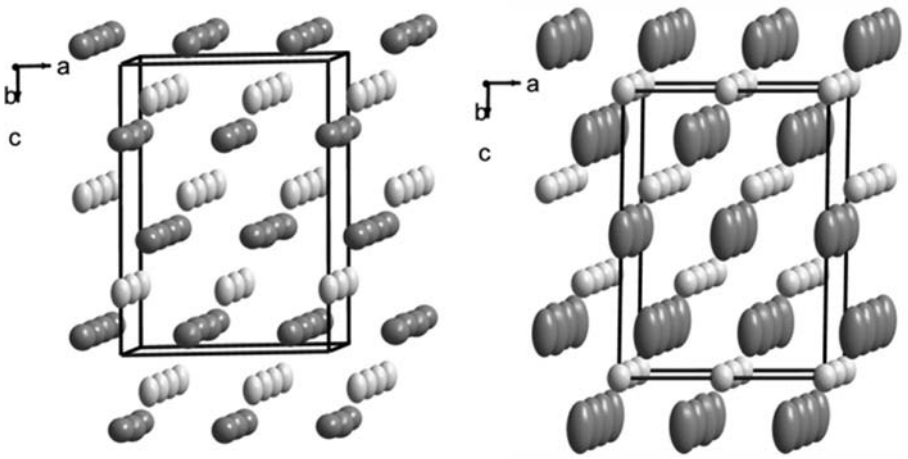

Figure 12. Representations of the structure solution of α-GeTe with a = 8.396(2) Å and c = 10.637(3) in $R3m$ (left) and $R\bar{3}m$ (right). The displacement ellipsoids are plotted at a 90% probability.

°C. The solvent was found to play a critical role on the reaction mechanism, since highly stoichiometric GeTe octahedra were obtained only in the presence of primary and secondary amines. Oleylamine has to be considered rather as a reagent, which strongly affects the chemistry of the whole reaction, than as a simple capping agent. In contrast, reactions in DIPB occurred with elimination of Et_3SiCl and subsequent formation of agglomerated GeTe particles, whereas reactions in tri-*n*-octylamine and 1-hexadecanethiol produced elemental tellurium. The presence of protic, strongly coordinating solvents is essential for the formation of GeTe particles with defined chemical composition, size, and shape. In the presence of an excess of $Te(SiEt_3)_2$, GeTe particles decorated with Te nanowires were obtained. The Te nanowires can be removed by washing the particles with TOP. A single-crystal and powder X-ray determination proved that GeTe crystallizes in the acentric space group $R3m$.

■ ASSOCIATED CONTENT

Supporting Information

CIF files giving crystallographic data for GeTe as well as details on the in situ ^{1}H NMR, TGA, and TEM studies are available free of charge via the Internet at http://pubs.acs.org.

■ AUTHOR INFORMATION

Corresponding Author

*E-mail: stephan.schulz@uni-due.de.

Author Contributions

All authors have given approval to the final version of the manuscript.

Notes

The authors declare no competing financial interest.

■ ACKNOWLEDGMENTS

S.S. and A.V.M. would like to thank the Mercator Foundation for support in the project SMILE.

■ REFERENCES

(1) For a recent review article see: Gao, M.-R.; Xu, Y.-F.; Jiang, J.; Yu, S.-H. *Chem. Soc. Rev.* **2013**, *42*, 2986−3017.
(2) Welnic, W.; Botti, S.; Reining, L.; Wuttig, M. *Phys. Rev. Lett.* **2007**, *98*, 236403-1−4.
(3) Welnic, W.; Pamungkas, A.; Detemple, R.; Steimer, C.; Blügel, S.; Wuttig, M. *Nat. Mater.* **2006**, *5*, 56−62.
(4) Wuttig, M.; Lüsebrink, D.; Wamwangi, D.; Wenic, W.; Gilleßen, M.; Dronskowski, R. *Nat. Mater.* **2007**, *6*, 122−128.
(5) Lencer, D.; Salinga, M.; Wuttig, M. *Adv. Mater.* **2011**, *23*, 2030−2058.
(6) See also: *Phase Change Materials: Science and Application*; Raoux, S.; Wuttig, M., Eds.; Springer: New York, 2009.
(7) Wuttig, M.; Yamada, N. *Nat. Mater.* **2007**, *6*, 824−832.
(8) Snyder, J.; Toberer, E. S. *Nat. Mater.* **2008**, *7*, 105−114.
(9) Raoux, S.; Welnic, W.; Ielmini, D. *Chem. Rev.* **2010**, *110*, 240−267.
(10) Polking, M. J.; Han, M.-G.; Yourdkhani, A.; Petkov, V.; Kisielowski, C. F.; Volkov, V. V.; Zhu, Y.; Caruntu, G.; Alivisatos, A. P.; Ramesh, R. *Nat. Mater.* **2012**, *11*, 700−709.
(11) Caldwell, M. A.; Jeyasingh, R. G. D.; Wong, H.-S. P.; Milliron, D. J. *Nanoscale* **2012**, *4*, 4382−4392.
(12) Xiao, G.; Wang, Y.; Ning, J.; Wei, Y.; Liu, B.; Yu, W. W.; Zou, G.; Zou, B. *RSC Adv.* **2013**, *3*, 8104−8130.
(13) Bruns, G.; Merkelbach, P.; Schlockermann, C.; Salinga, M.; Wuttig, M.; Happ, T. D.; Philipp, J. B.; Kund, M. *Appl. Phys. Lett.* **2009**, *95*, 043108-1−3.
(14) Lankhorst, M. H. R.; Ketelaars, B.; Wolters, R. A. M. *Nat. Mater.* **2005**, *4*, 347−352.
(15) Steigmeier, E. F.; Harbeke, G. *Solid State Commun.* **1970**, *8*, 1275−1279.
(16) Wood, C. *Rep. Prog. Phys.* **1988**, *51*, 459−539.
(17) Raoux, S.; Rettner, C. T.; Jordan-Sweet, J. L.; Kellock, A. J.; Topuria, T.; Rice, P. M.; Miller, D. C. *J. Appl. Phys.* **2007**, *102*, 094305−1−8.
(18) Zhang, Y.; Raoux, S.; Krebs, D.; Krupp, L. E.; Topuria, T.; Caldwell, M. A.; Milliron, D. J.; Kellock, A.; Rice, P. M.; Jordan-Sweet, J. L.; Wong, H.-S. P. *J. Appl. Phys.* **2008**, *104*, 074312-1−5.
(19) Martens, H. C. F.; Vlutters, R.; Prangsma, J. C. *J. Appl. Phys.* **2004**, *95*, 3977−3983.
(20) Wang, W. J.; Shi, L. P.; Zhao, R.; Lim, K. G.; Lee, H. K.; Chong, T. C.; Wu, Y. H. *Appl. Phys. Lett.* **2008**, *93*, 043121−1−3.
(21) Raoux, S.; Shelby, R. M.; Jordan-Sweet, J. L.; Munoz, B.; Salinga, M.; Chen, Y.-C.; Shih, Y.-H.; Lai, E.-K.; Lee, M.-H. *Microelectron. Eng.* **2008**, *85*, 2330−2333.
(22) Sun, X.; Yu, B.; Ng, G.; Meyyappan, M. *J. Phys. Chem. C* **2007**, *111*, 2421−2425.
(23) Caldwell, M. A.; Raoux, S.; Wang, R. Y.; Wong, H. S. P.; Milliron, D. J. *J. Mater. Chem.* **2010**, *20*, 1285−1291.
(24) Vaughn, D. D., II; Schaak, R. E. *Chem. Soc. Rev.* **2013**, *42*, 2861−2879.
(25) Lee, M.-K.; Kim, T. G.; Ju, B.-K.; Sung, Y.-M. *Cryst. Growth Des.* **2009**, *9*, 938−941.

(26) Jennings, A. T.; Jung, Y.; Engel, J.; Agarwal, R. *J. Phys. Chem. C* **2009**, *113*, 6898−6901.
(27) Arachchige, I. U.; Soriano, R.; Malliakas, C. D.; Ivanov, S. A.; Kanatzidis, M. C. *Adv. Funct. Mater.* **2011**, *21*, 2737−2743.
(28) Polking, M. J.; Urban, J. J.; Milliron, D. J.; Zheng, H.; Chan, E.; Caldwell, M. A.; Raoux, S.; Kisielowski, C. F.; Ager, J. W.; Ramesh, R.; Alivisatos, A. P. *Nano Lett.* **2011**, *11*, 1147−1152.
(29) Polking, M. J.; Zheng, H. M.; Ramesh, R.; Alivisatos, A. P. *J. Am. Chem. Soc.* **2011**, *133*, 2044−2047.
(30) Tuan, H. Y.; Korgel, B. A. *Cryst. Growth Des.* **2008**, *8*, 2555−2561.
(31) Buck, M. R.; Sines, I. T.; Schaak, R. E. *Chem. Mater.* **2010**, *22*, 3236−3240.
(32) Murray, C. B.; Norris, D. J.; Bawendi, M. G. *J. Am. Chem. Soc.* **1993**, *115*, 8706−8715.
(33) Schulz, S.; Andruh, M.; Pape, T.; Heinze, T.; Roesky, H. W.; Häming, L.; Kuhn, A.; Herbst-Irmer, R. *Organometallics* **1994**, *13*, 4004−4007.
(34) Corrigan, J. F.; Fenske, D. *Angew. Chem., Int. Ed.* **1997**, *36*, 1981−1983.
(35) DeGroot, M. W.; Cockburn, M. W.; Workentin, M. S.; Corrigan, J. F. *Inorg. Chem.* **2001**, *40*, 4678−4685.
(36) Dehnen, S.; Eichhöfer, A.; Fenske, D. *Eur. J. Inorg. Chem.* **2002**, *2*, 279−317.
(37) For a review article see: Dehnen, S.; Eichhöfer, A.; Corrigan, J. F.; Fenske, D. In *Nanoparticles−From Theory Applications*, 2nd ed.; Schmid, G., Ed.; Wiley: Weinheim, 2010.
(38) Pore, V.; Hatanpää, T.; Ritala, M.; Leskelä, M. *J. Am. Chem. Soc.* **2009**, *131*, 3478−3480.
(39) Pore, V.; Knapas, K.; Hatanpää, T.; Sarnet, T.; Kemell, M.; Ritala, M.; Leskelä, M.; Mizohata, K. *Chem. Mater.* **2011**, *23*, 247−254.
(40) Zastrow, S.; Gooth, J.; Boehnert, T.; Heiderich, S.; Toellner, W.; Heimann, S.; Schulz, S.; Nielsch, K. *Semicond. Sci. Technol.* **2013**, *28*, 035010-1−6.
(41) Kim, M. H.; Gupta, G.; Kim, J. *RSC Adv.* **2013**, *3*, 288−292.
(42) Buck, M. R.; Biacchi, A. J.; Popczun, E. J.; Schaak, R. E. *Chem. Mater.* **2013**, *25*, 2163−2171.
(43) Detty, M. R.; Seidler, M. D. *J. Org. Chem.* **1982**, *47*, 1354−1356.
(44) Sheldrick, G. M. *Acta Crystallogr., Sect. A* **1990**, *46*, 467−473.
(45) Sheldrick, G. M. *SHELXL-97, Program for the Refinement of Crystal Structures*; University of Göttingen: Göttingen, Germany, 1997 (see also: Sheldrick, G. M. *Acta Crystallogr., Sect. A* 2008, *64*, 112−122).
(46) Knapas, K.; Hatanpää, T.; Ritala, M.; Leskelä, M. *Chem. Mater.* **2010**, *22*, 1386−1391.
(47) Mourdikoudis, S.; Liz-Marzán, L. M. *Chem. Mater.* **2013**, *25*, 1465−1476.
(48) Hollemann; Wiberg. *Lehrbuch der Anorganischen Chemie*, 102; Auflage, deGruyter: Berlin, 2007.
(49) Chung, H.-S.; Jung, Y.; Kim, S. C.; Kim, D. H.; Oh, K. H.; Agarwal, R. *Nano Lett.* **2009**, *9*, 2395−2401.
(50) Shevchik, N. J.; Tejeda, J.; Langer, D. W.; Cardona, M. *Phys. Rev. Lett.* **1973**, *30*, 659−662.
(51) Tomaszewski, P. E. In Structural Phase Transitions in Crystals. I. Database. *Phase Transitions: A Multinational Journal* **1992**, *38:3*, 127−220, DOI: 10.1080/01411599208222899.
(52) Grier, D.; McCarthy, G.; Seidler, D.; Boudjouk, P. North Dakota State Univ., Fargo, ND, USA, ICDD Grant-in-Aid JCPDS, 1993, 00-047-1047
(53) Chopra, K. L.; Bahl, S. K. *J. Appl. Phys.* **1969**, *40*, 4171−4178.
(54) Andrikopoulos, K. S.; Yannopoulos, S. N.; Voyiatzis, G. A.; Kolobov, A. V.; Ribes, M.; Tominaga, J. *J. Phys.: Condens. Matter* **2006**, *18*, 965−979.
(55) Gervacio Arciniega, J. J.; Prokhorov, E.; Espinoza Beltran, F. J.; Trapaga, G. Crystallization of Ge:Sb:Te Thin Films for Phase Change Memory Application. *Crystallization−Science and Technology*; Andreeta, M., Ed.; InTech, 2012; DOI: 10.5772/35577. Available from http://www.intechopen.com/books/crystallization-science-and-technology/crystallization-of-gesbte-thin-films-for-phase-change-memory.
(56) Bahl, S. K.; Chopra, K. L. *J. Appl. Phys.* **1969**, *40*, 4940−4947.
(57) Bahl, S. K.; Chopra, K. L. *J. Appl. Phys.* **1970**, *41*, 2196−2212.
(58) Chattopadhyay, T.; Boucherle, J. X.; von Schnering, H. G. *J. Phys. C: Solid State Phys.* **1987**, *20*, 1431−1440.
(59) Goldak, J.; Barrett, C. S.; Innes, D.; Youdelis, W. *J. Chem. Phys.* **1966**, *44*, 3323−3325.
(60) Matsunaga, T.; Kojima, R.; Yamada, N.; Kifune, K.; Kubota, Y.; Tabata, Y.; Takata, M. *Inorg. Chem.* **2006**, *45*, 2235−2241.
(61) Nonaka, T.; Ohbayashi, G.; Toriumi, Y.; Mori, Y.; Hashimoto, H. *Thin Solid Films* **2000**, *370*, 258−261.
(62) Wiedemeier, H.; Siemers, P. A. *High Temp. Sci.* **1984**, *17*, 395−408.
(63) Wiedemeier, H.; Siemers, P. A. *Z. Anorg. Allg. Chem.* **1977**, *431*, 299−304.
(64) Abrikosov, N. Kh.; Avilov, E. S.; Karpinskii, O. G.; Radkevich, O. V.; Shelimova, L. E. *Inorg. Mater.* **1984**, *201*, 20−24.
(65) Parker, S. G.; Pinnell, J. E.; Swink, L. N. *J. Mater. Sci.* **1974**, *9*, 1829−1832.
(66) Barret, C.; Massalski, T. B. In *Structure of Metals*; Pergamon Press: Oxford, 1980.